MJFAS MALAYSIAN JOURNAL OF FUNDAMENTAL AND APPLIED SCIENCES
PRINT ISSN: 2289-5981 | ONLINE ISSN: 2289-599X

RESEARCH ARTICLE

Zeolite templated carbon: Preparation, characterization and performance as filler material in co-polyimide membranes for CO_2/CH_4 separation

Triyanda Gunawan [a], Taufik Qodar Romadiansyah [a], Rika Wijiyanti [a], Wan Norharyati Wan Salleh [b, c], Nurul Widiastuti [a, *]

[a] Department of Chemistry, Faculty of Science, Institut Teknologi Sepuluh Nopember, Sukolilo, Surabaya 60111, Indonesia
[b] School of Chemical and Energy Engineering, Faculty of Engineering, Universiti Teknologi Malaysia, 81310 UTM Johor Bahru, Malaysia
[c] Advanced Membrane Technology Research Centre (AMTEC), Universiti Teknologi Malaysia, 81310 UTM Johor Bahru, Malaysia
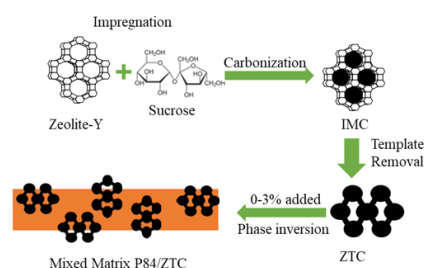
* Corresponding author: nurul_widiastuti@chem.its.ac.id

Graphical abstract

Abstract

Zeolite templated carbon (ZTC), a structurally unique carbon material was used as new fillers for the preparation of composite polymeric membrane derived from BTDA-TDI/MDI (P84) co-polyimide. The thermal stability of membrane, the structure evolution, morphology and topology, as well as gas separation performance of modified membranes were investigated. Zeolite-Y, a hard template for ZTC, was synthesized via hydrothermal method. The ZTC was synthesized via impregnation of sucrose as carbon precursor into zeolite pore and followed by carbonization at 800°C. The zeolite template was removed through acid treatment to obtain ZTC, which was used as fillers for membrane preparation. The membrane was prepared using P84 co-polyimide as membrane precursor via phase inversion process. Synthesized materials were characterized using SEM, XRD, N_2 adsorption-desorption isotherm and TEM. The thermal stability of membrane was improved by the addition of ZTC. As the result of ZTC loading into P84 co-polyimide membrane, the gas permeability of CO_2 increased thirty-four times, as well as the CO_2/CH_4 selectivity boosted from 0.76 to 5.23. The ordered pore structure in ZTC plays important role in increasing the permeability and selectivity performances of the P84 co-polyimide membrane.

Keywords: Mixed matrix membrane, P84 co-polyimide, zeolite templated carbon, CO_2 separation

INTRODUCTION

Separating gas via membrane technology is the most energy efficient and has many opportunities for development, thus making this field of research grows fast around 15% annually. A very exciting field for both scientifically and industrially is gas separation using polymeric membrane. In current industrial membrane gas separation technologies, both glassy and rubbery based polymer are widely used. The most popular rubbery polymers are ethylene oxide [1] and amide copolymer [2,3]. As well, polyimides [4–6], polysulfone [7,8], and polyamide imide [9] are the most referred glassy polymers. Polyimide based polymers are one of the most used polymers for preparing gas separation membrane. Polyimides have good thermal properties (Tg~300°C) and they can be easily prepared in various modules such as flat, tubular support and hollow fiber. Furthermore, they are affordable cand provide good mechanical properties. In addition, these types of polymers are good for preparing carbon membrane [10–13].

Polymeric membrane for gas separation has a lot of drawbacks, especially in the trade-off between permeability and selectivity [5]. To overcome that drawbacks, many researchers are tried to fix that by blending polymers [14] and preparing composite membrane [2,4,15,16]. Composite membrane is polymer membrane incorporated with inorganic materials, has been proved to be a most effective and easy way to improve the membrane performance [17]. The idea is to combine the processability of polymeric membrane with the selective adsorption and diffusion properties of inorganic molecular sieve. By increasing or limiting the diffusion of gases in the membrane, it should improve the permselectivity. Nanoporous materials such as silica [18], zeolites [19], inorganic oxide [2] and carbon nanotube [4], have been reported to form composite membrane. However, there are still technical challenges to be met such as avoiding pin hole formation and incompatability issue with polymer precursor.

In this study, zeolite templated carbon (ZTC), a structurally unique carbon material, was prepared by impregnation of sucrose into zeolite-Y pores. ZTC was used as filler material into BTDA-TDI/MDI (P84) co-polyimide membrane, which prepared by phase inversion process. Our motive in utilizing this material as filler was due to the benefits of material such as high surface area, high microporosity, and ordered pore structure [20–22]. With such characteristics, it is predicted that by adding ZTC into polymer matrix, it will improve the gas permeabiltiy due to ordered free main path (ordered pore) and gas selectivity due to high microporosity. As a result, this material will fits the required properties for gas separation membrane. However, there is no reported research related about this material utilized as a membrane filler yet. Thus, this research carried out preparation and fabrication of ZTC/polymeric membrane composite. A series of ZTC/P84 composite membrane loaded with ZTC content between 1-3 wt% was prepared by phase inversion method. Detailed characterizations on morphology

(SEM), thermal stability (TGA), crystalline structure (XRD), topology (AFM) and functional group (FTIR) have been conducted to understand the properties of nanocomposite polymeric membranes.

EXPERIMENTAL

Materials

Materials used for synthesizing ZTC were sulfuric acid (H_2SO_4, 98%) was purchased from Merc, sodium aluminate ($NaAlO_2$, Sigma Aldrich) was used as aluminate and sodium source for zeolite formation, sodium silicate (Na_2SiO_3, Sigma Aldrich) was used as silicate and sodium source, and sodium hydroxide (99% NaOH, pellet) was purchased from Sigma Aldrich for additional sodium source and as counter ion of zeolite. Sucrose (98%, Fluka) was used as carbon source for ZTC.

For the membrane preparation, Polyimide BTDA-TDI/MDI (P84) purchased from HP Polymer GmbH was selected as polymer precursor. P84 was dried at 100°C overnight to remove any moisture prior to membrane preparation. N-methyl-2-pyrrolidone (NMP) purchased from Merck was selected as solvent.

Synthesis of ZTC

The overall synthesis method for preparing zeolite, ZTC and composite membrane can be seen in Figure 1. Zeolite Y was synthesized via hydrothermal of zeolite seed crystals. The molar composition of the gel was 1.0 $NaAlO_2$: 18 Na_2SiO_3: 1.75 NaOH: 23.33 H_2O. The gel was prepared by dissolving NaOH and $NaAlO_2$ into DI water. The solution was stirred at room temperature until homogenous aluminate solution was obtained. Then, Na_2SiO_3 was added drop wisely into the aluminate solution and stirred for 20 minutes. The solution was then moved into stainless steel autoclave and aged for 1 day. The hydrothermal reaction was conducted in an oven at 100°C for 7h. The zeolite was then filtered and washed until pH of filters reached <9 and followed by drying at 110°C for 24h. White powder of zeolite-Y was obtained and stored in a desiccator for the next purpose.
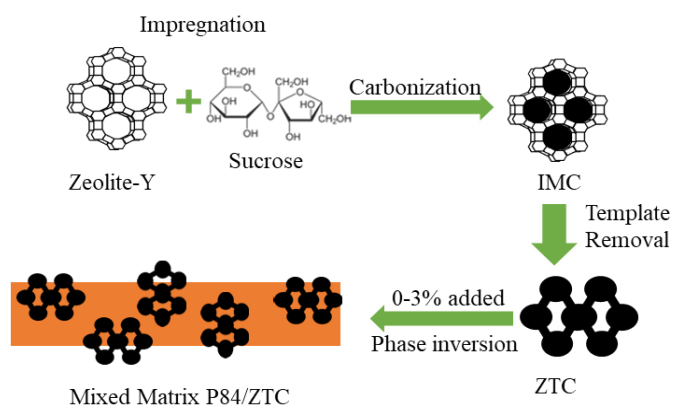

Figure 1 Schematic diagram of impregnated zeolite-carbon composite (IMC), ZTC and membrane preparation.

Prepared zeolite-Y was used as template for zeolite templated carbon (ZTC). ZTC was synthesized via impregnation method. Zeolite-Y was degassed at 200°C for 4h inside a tubular furnace with the heating rate of 1°C/min to remove any adsorbed gasses prior to impregnation process. The mass ratio of zeolite-Y and sucrose was 1:1.25 [1]. The impregnation process was carried out by dissolving sucrose into 50 mL H_2SO_4 0.35M to facilitate the dehydration process of sucrose. Then, it was followed by the addition of degassed zeolite Y into sucrose solution and stirred at 250 rpm for 72h in room temperature. The solution was then filtered and its residue (impregnated zeolite) was moved into tubular holder prior to carbonization process. The carbonization process was conducted inside a tubular furnace at 800°C for 4h with heating rate of 2°C/min and under N_2 flow of 30 cm^3/min. The carbonization product was then ground to obtain fine powder. The carbonization product was immersed in 5% hydrofluoric acid (HF) for 1h to break the Si bonding in zeolite, followed by

refluxing at 60°C in concentrated hydrochloric acid (HCl) to remove the Al phase in zeolite and finally immersed in 48% HF for 1h to completely remove zeolite framework [1]. The ZTC obtained was then stored inside desicator for future treatment.

Synthesis of P84/ZTC mixed matrix membrane

BTDA-TDI/MDI (P84) and ZTC were dried at 80°C for 24h before the membrane preparation took place to remove moisture. Dope solution was consisted of 12 wt% P84/88 wt% NMP. A total of 0-3 wt% of ZTC to P84 co-polyimide mass ratio was dispersed in 88% NMP by sonication for 30 minutes. A total 12 wt% of P84 was added to the mixture slowly and stirred with mechanical stirrer for 24h at 80°C. The dope solution was then sonicated to remove the existed bubble. The bubble-free dope solution was directly casted onto the clean glass plate to fabricate composite membrane, followed by immersion into water to perform the phase inversion process. The membranes were then dried at room temperature for 24h to remove the remained water.

Material characterization

X-Ray Diffractogram (XRD) was utilized to confirm the structure formation of Zeolite-Y and ZTC. The pore properties of ZTC were measured using Surface Area and Porosity Analyzer (Micromeritics, ASAP 2020). The gas used for adsorptive analysis was N_2 and the analysis temperature was at -195°C. The morphology of each samples was observed using Scanning Electron Microscope (Hitachi, TM 3000) with a potential of 15kV and samples were coated with platinum. The membrane thermal stability was characterized using thermal gravimetric analysis (TGA). The alterations in sample weight during the continuous heating process were recorded by TGA. The samples were heated from room temperature to 900°C at heating rate of 10°C/min and nitrogen flow rate of 20 ml/min.

The pore size distribution (PSD) of ZTC was calculated using SAIEUS software with 2D-NLDFT. The NLDFT graph was obtained by plotting pore diameter against different pore volumes obtained from N_2 adsorption desorption isotherm. An average pore radius was evaluated by using Equation 1.

$$\bar{r}_p = \frac{2V_p}{S} \qquad (1)$$

where, S is the surface area and V_p is the pore volume, which were obtained from N_2 physisorption.

The membrane permeation performance was conducted by cutting the membrane into circle shape membrane with diameter of 5.7 cm. The single gas permeability was conducted at room temperature and pressure of 4 bar. The data measurement was taken by measuring the time for permeate gas required to reach 10 mL. The gas volume was measured using bubble flow meter. The measurement was repeated 10 times. The permeability (cm^3 (STP) cm/cm^2 s cmHg) was calculated using Equation 1.

$$P_i = \left(\frac{Q \times l}{\Delta P \times A} \right) \qquad (2)$$

where, P_i is the permeability of membrane for gas *i* in the standard unit of Barrer (1 Barrer = 10^{-10} cm^3(STP)cm/cm^2 s cmHg), Q is the volumetric gas flow rate at standard temperature and pressure (cm^3 (STP)/s), *l* is the membrane selective layer thickness (cm), Δp is the different pressure between feed and system (cmHg), A is effective surface area of membrane (cm^2).

The selectivity of membrane was calculated using Equation 2.

$$\alpha_{i/j} = \frac{P_i}{P_j} \qquad (3)$$

The single gas test apparatus scheme was shown in Figure 2.

RESULTS AND DISCUSSION

Physicochemical properties of ZTC

Figure 3a shows the diffractogram pattern of the ZTC, while inset Figure 3b shows the diffractogram patterns of synthesized zeolite-Y

and the standard, JCPDS No. 39-1380. The diffractogram pattern of synthesized zeolite-Y has the same pattern as standard's, indicating the formation of highly arranged zeolite crystal. ZTC diffractogram pattern shows typical amorphous material since the zeolite peaks at 2θ of $6°$; $10°$; $11.8°$; $15.5°$; $18.6°$; $20.2°$; $23.5°$; $26.9°$; $29.4°$; $30.5°$; $31.2°$; $32.3°$; $33.9°$; $34.5°$; $37.6°$; and $41.1°$ were not appeared. This indicates that acid treatment successfully removes zeolite from the composite, leaving the templated carbon behind. The broad peak at $2\theta \sim 25°$ in Figure 3a was corresponded to the (002) plane, which has low intensity that indicated for few graphitic phases formed in the synthesized templated carbon [2]–[4]. The peak at around $2\theta \sim 45°$ was assigned to the (100) diffraction of graphitic carbon [2]. Those peaks indicated a quasi-crystalline carbon structure. The peak at 2θ of $6°$, which corresponded to the (111) planes of zeolite-Y was not clearly seen in this study. This indicates that the structural ordering of the sample is low, which not observed in previous study [2].
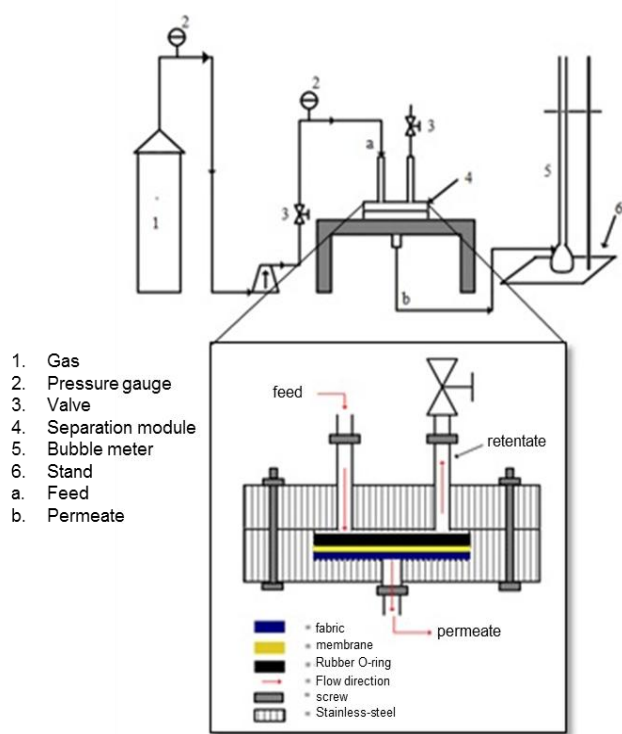

Figure 2 Single gas permeation apparatus.

1. Gas
2. Pressure gauge
3. Valve
4. Separation module
5. Bubble meter
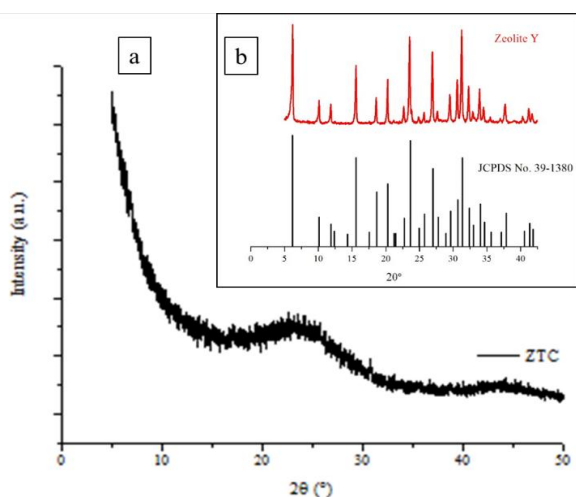6. Stand
a. Feed
b. Permeate

Figure 3 Diffractogram pattern of (a) ZTC and (b) Inset image of comparison JCPDS No. 39-1380 vs synthesized zeolite-Y.

Figure 4 shows the TEM image of ZTC. TEM image reveals that the ZTC particle consisted of a thick graphite core surrounded by thin graphite shell (external carbon surface). It is suggested that, this thin external carbon surface comes from the sucrose particle that did not enter the zeolite pore. The TEM image shows that, even though ZTC has amorphous diffractogram, the particle structure was similar to crystalline-like material. This indicates that ZTC successfully replicates the zeolite structure. Same result also observed in previously reported work by Choi et al. (2015).
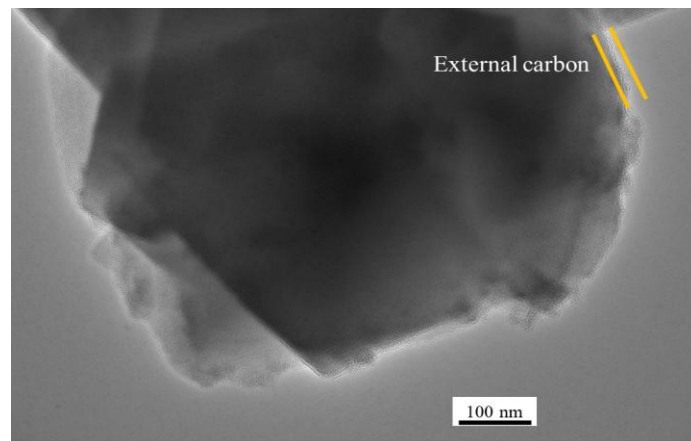

Figure 4 TEM image of ZTC particles.

The SEM image in Figure 5a shows octahedral crystal of zeolite-Y, a typical morphology of zeolite-Y which indicated that the crystal formation through gel method is well formed.

Figure 5b reveals that ZTC prepared here has two main morphologies, one is the replication of zeolite template (marked with rectangle) and another one is amorphous carbon (marked with circle) which is in agreement with diffractogram data. The particle size of ZTC was smaller compared to zeolite-Y particle, ranging from 400 to 500 nm compared to ranging 900 to 1000 nm, respectively.
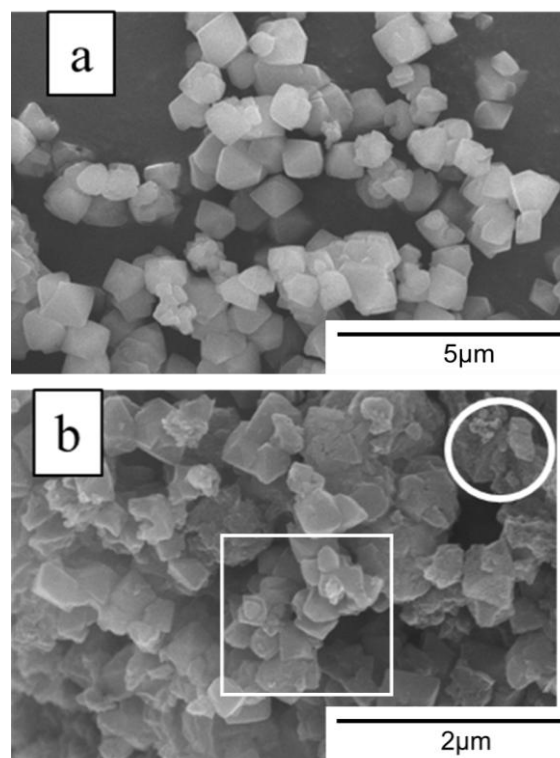

Figure 5 SEM image of a) Zeolite Y and b) ZTC.

The pore size distribution of ZTC was plotted in Figure 6. From the graph, the pore distribution was ranged from 0.5-10 nm. The

mesoporous site comes from the graphitic phase that covered ZTC particle. Moreover, from the N_2 adsorption-desorption measurement, the surface area of prepared ZTC was 1254.38 m^2/g and total pore volume was 0.950 cc/g. The surface area of ZTC prepared in this study is slightly bigger than previously reported impregnated ZTC pyrolyzed at 900°C from glucose [6] and furfuryl alcohol (FA) [7], which were 1222 and 1245, respectively. The average pore size of ZTC was calculated using Equation 1 and assumption of the cylindrical pore. The average pore size of the prepared ZTC was 1.5 nm, which in the range of micropore.
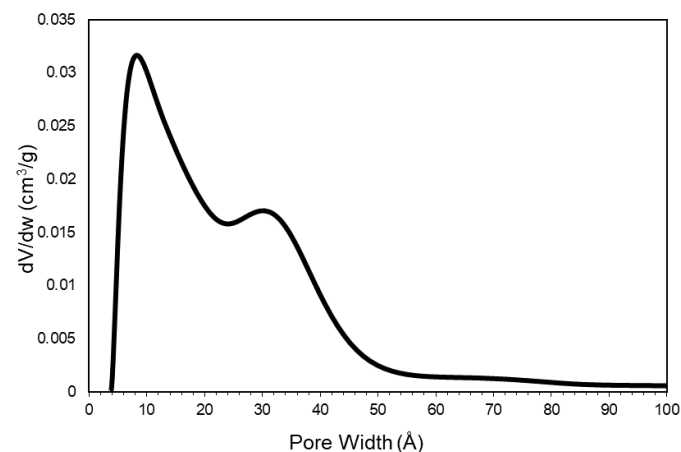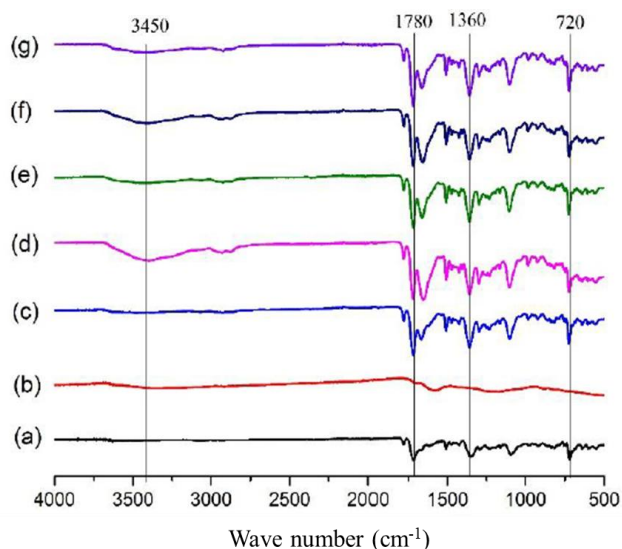

Figure 6 Pore size distribution of ZTC.

Figure 7 FTIR image of (a) P84 co-polyimide powder, (b) ZTC, (c) Neat Membrane, (d) P84/ZTC 1% before gas permeation test, (e) P84/ZTC 1% after gas permeation test, (f) P84/ZTC 3% before gas permeation test, (g) P84/ZTC 3% after gas permeation test.

Physicochemical properties of P84/ZTC mixed matrix membrane

The structure of the prepared membrane was characterized using Fourier Transform Infrared (FTIR, Figure 7) and X-ray Diffractogram (XRD, Figure 8). As seen in Figure 7, there were observed peaks at 720 cm^{-1} corresponded to C=O, 1360 cm^{-1} corresponded to C-N and 1700 cm^{-1} corresponded to C=O asymmetric in FTIR spectra of all membranes. There was no significant difference in all prepared membrane. However, in both 1 and 3 wt% loaded ZTC membranes before gas permeation, broad peak at 3450 cm^{-1} was appeared that corresponded to the OH from moisture. The intensity of this peak plummeted at higher ZTC loading. This is due to hydrophobic properties of ZTC which reduce the affinity towards water molecule. On the other hand, the spectra of membrane after gas test showed no difference to the structure of membrane, indicating that there is no chemical interaction between membrane and permeate gas. The XRD

pattern shows a typical amorphous structure. After an addition of 1 wt% of ZTC, the d-spacing in broad peak at 2θ around 17° was increased from 4.99 Å to 5.22 Å for neat and P84/ZTC1%, respectively. The increase in *d*-spacing indicates that the polymer matrix is expanded to provide enough space for ZTC particle. Moreover, it can be predicted that the positive shift of *d*-spacing indicates that there will be an enhanced permeability of the membrane due to increased of free volume distribution in the polymer matrix [8]. In contrast, this broad peak was not observed at higher ZTC loading, in this case P84/ZTC3%, and the broad peak was similar to the ZTC peak. This indicates that at higher ZTC loading, the adhesion forces between P84 co-polyimide and ZTC particle get stronger. Thus, resulting in P84 co-polyimide matrix to cover the ZTC particle in the fit and proper manner.
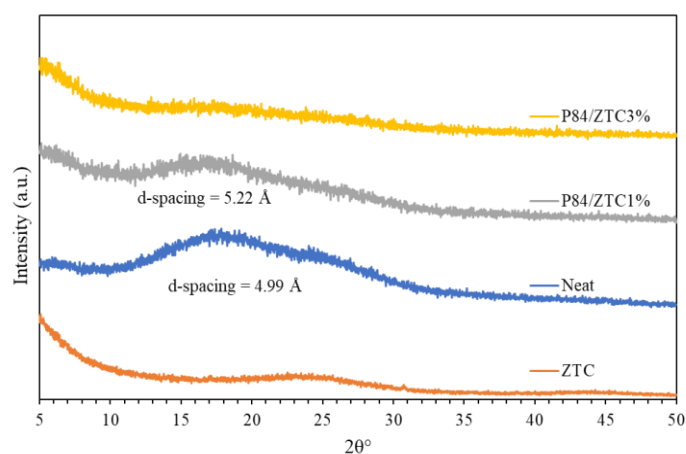

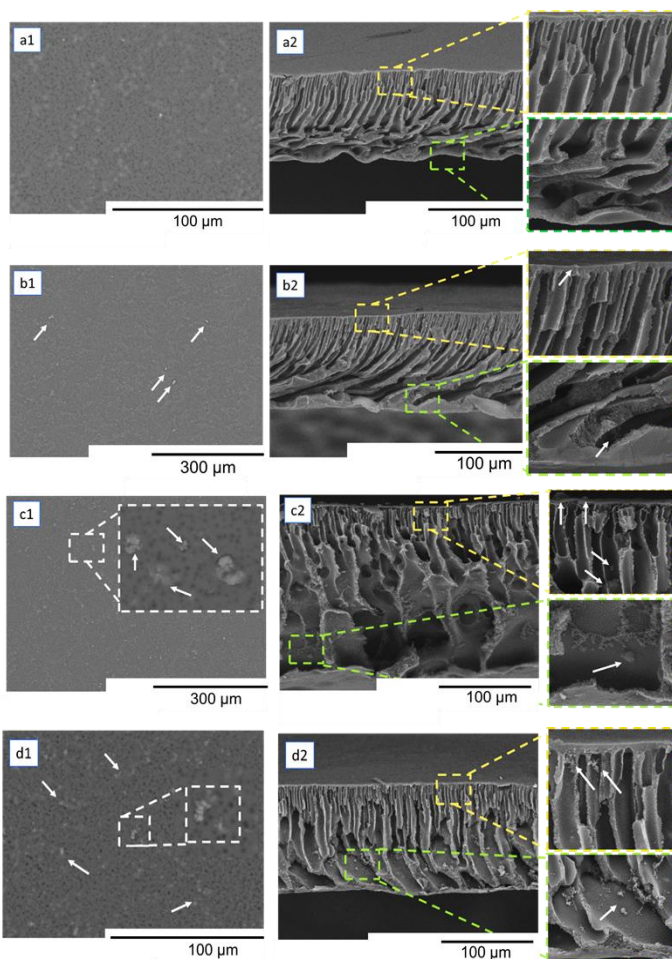**Figure 8** The Diffractogram of the prepared mixed matrix membrane.
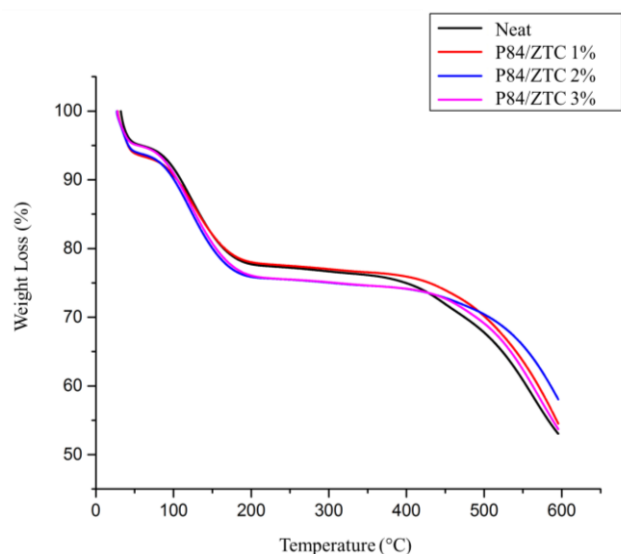

Figure 9 SEM image of a) Neat, b) P84/ZTC 1%, c) P84/ZTC 2%, d) ZTC 3%. The number of 1 and 2 correspond to the surface and cross-section, respectively.

Table 1 Dense layer thickness of each prepared membrane.

Membrane	Dense layer Thickness (µm)
Neat	0.891
P84/ZTC1%	1.426
P84/ZTC2%	1.378
P84/ZTC3%	1.275

Table 2 Starting decomposition temperature and total residual solvent from each membrane.

| Membrane	Decomposition Temperature (°C)	Residual Solvent (%)
Neat	380	16.5
P84/ZTC 1%	388	15
P84/ZTC 2%	395	16.6
P84/ZTC 3%	390	18.2

The morphological structures of the prepared membranes were shown in the Figure 9. As can be seen in Figure 9, the neat membrane has smooth surface, while the composite membrane showed rough surface due to the ZTC appeared on the surface, marked with white spot. This white spot spread throughout the membrane surface, indicating well dispersed composition. The white spot spread wider together with the increment of ZTC loading. According to the cross-section image, all of the prepared membranes consisted of two layers, selective dense layer on top and finger-like macrovoid at bottom. The ZTC loading does not influence much on amount of total macrovoid. However, the selective layer thickness was decreased as the ZTC loading was increased, as listed in Table 1, which is in agreement with the diffractogram data. High ZTC loading tends to has stronger adhesion force, which pulls the polymer matrix and makes the selective layer thinner. Additionally, around the agglomeration of ZTC particle as observed in Figure 11 c1 and d1, there were interphase voids around the agglomerated ZTC particle. It is predicted that the interphase voids will increase the permeability but reduce the selectivity.

Figure 10 shows the thermogravimetric analysis (TGA) of prepared membranes. The first weight loss below 100°C was due to the evaporation of adsorbed water molecule. The second weight loss in the temperature range of 100 to 200°C was due to the evaporation of solvent NMP (T_b of NMP= 202-204°C). The final weight loss stage, started at temperature around 350°C was corresponded to the P84 decomposition matrix. The ZTC slightly improved the thermal stability of the membrane, as listed in Table 2. It seems that ZTC acts as heat receptor during the process. As the amount of ZTC increases, the starting decomposition of the membrane increases as well. This is due to more ZTC dispersed throughout the membrane surface, helping to reduce the heat that directly received by the polymer body. However, at addition 3 wt% of ZTC, the membrane thermal resistant was slightly reduced compared to the 2 wt% of ZTC. The reduction on P84/ZTC3% membrane is due to the agglomeration of ZTC, consequently it will reduce the dispersion of fillers in the membrane surface and reduce the heat distribution on the membrane surface. Since the membrane did not undergo any post treatment except drying, the residual solvent was observed in all of prepared membranes. This residual solvent content improves together with the increment in ZTC loading. The natural properties of ZTC as organophilic like other carbon materials lead to the increased affinity towards organic solvent, in this case is NMP [9].

The topology of each membrane was shown in Figure 11 and the roughness value was listed in Table 3. The neat membrane has the smoothest surface compared to all, indicated by the lowest value of R_a. The surface of the membrane becomes rougher as the ZTC loading increases. Moreover, in each ZTC loaded membrane, there was high peak ~50 nm in height correspond to the ZTC particle and this amount of peak increased together with the ZTC amount loaded. This indicates that the ZTC particle is successfully deposited on the membrane surface with good dispersion.
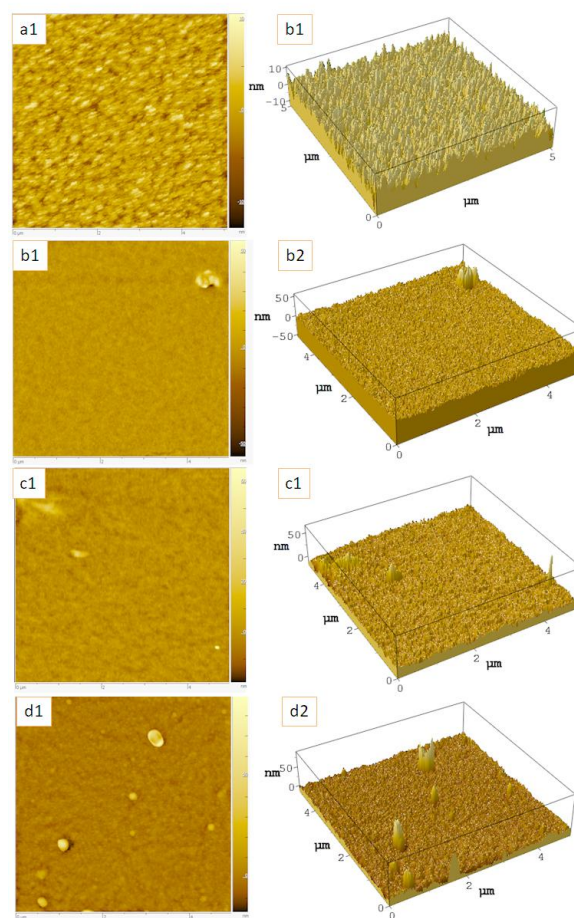
Figure 11 AFM image of a) Neat, b) P84/ZTC 1%, c) P84/ZTC 2%, d) P84/ZTC 3%.

Table 3 The surface roughness value of the prepared membrane.

Membrane	Ra (nm)	Rms (nm)
Neat	1.76	2.22
P84/ZTC 1%	2.13	3.12
P84/ZTC 2%	2.33	3.26
P84/ZTC 3%	2.44	4.69

Single gas permeation performance

The single gas permeation result and the ideal gas selectivity were presented in Figure 12. As expected, the permeability of CH_4, which has kinetic diameter of 0.38 nm was slower than the permeability of CO_2, which has smaller kinetic diameter of 0.33 nm for all composite membranes. Compared to pure P84 membrane on previously reported paper [10], the ZTC incorporation increased the CO_2 permeability significantly, from 2.7 to 8.84±0.31 barrer.

Figure 10 TGA curve of all prepared membranes.

An interesting result of the permeabilities of both gasses were increased significantly as the ZTC loading was increased, according to linear relation as shown in Figure 12, which is predicted from the diffractogram result. The CO_2 permeabilities in membrane with ZTC loading of 1 wt%, 2 wt% and 3 wt% were 4.26±0.78, 7.70±0.44 and 8.84±0.31, respectively. The increment of ZTC loading made the selective area became thinner, from 1.43 to 1.38 to 1.16 µm for 1 wt% to 2 wt% to 3 wt% ZTC loading, respectively. Although, the CO_2 permeability was increased as the ZTC loading was increased, the selectivity trades off was still inevitable, as shown in Figure 12. The selectivities were decreased by 1.35 and 2.36 factors for ZTC loadings of 1 wt% to 2 wt% and 2 wt% to 3 wt%, respectively. The decrease in the selectivity is due to pin hole formation on the surface of the membrane from inperfect solution exchange during the phase inversion process. Moreover, at higher ZTC loading, the residual solvent, which was observed in the TGA analysis, was also get higher. This residual solvent will improve the permeability, solubility and diffusivity coefficients of the membrane.

Table 4 Separation performance of samples studied in this work and comparison with the previously reported work.

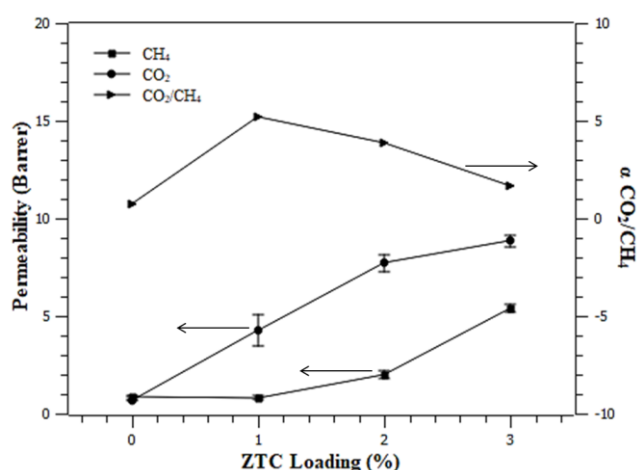| Samples	CH₄ (0.38 nm)	CO₂ (0.33 nm)	Ideal Selectivity CO₂/CH₄	Ref.
	Permeability (Barrer)	Permeability (Barrer)		
Neat	0.88±0.02	0.67±0.03	0.76	This work
P84/ZTC 1%	0.82±0.11	4.26±0.78	5.23	
P84/ZTC 2%	2.00±0.23	7.70±0.44	3.87	
P84/ZTC 3%	5.40±0.17	8.84±0.31	1.64	
P84 Hollow fiber	3.55	2.70	0.76	[10]
Matrimid/Zeolite 4A	4.25	9.36	2.2	[11]
PBNPI/MWCNT	0.74	2.18	2.95	[12]
SEBS/ZIF8	454.6	84.1	5.4	[13]
PSF/CIF (0.1)	0.26	1.31	5.03	[14]

Figure 12 The effect of ZTC loading towards CO_2 permeation and CO_2/CH_4 selectivity.

The residual solvent, which acts as a plasticizer will facilitate the movement of polymer segments and increases the gas permeability, solubility, and diffusivity coefficients. The increases in gas permeability, solubility and diffusivity are accompanied by a loss in selectivity. ZTC as a carbon material is inevitable to has organophilic properties, which leads these phenomena to occur. In this case, adding more ZTC content is unnecessary. However, this can be avoided by post treatment of the membrane. Sazali et. al. reported that immersion of methanol for 2h could remove the excess NMP in the membrane [15]. This also opens new challenge to modify ZTC material, so that

the material can maintain to keep the CH_4 permeability almost constant, while increase the permeability of CO_2.

Figure 13 shows the performance comparison of the prepared membrane to previously reported result. As can be seen in Figure 13, all of prepared membranes were below the Robeson upper bound 2008. This is quite understandable since the precursor used is P84 co-polyimide, which has performance below Robeson upper bound, but a very good precursor for carbon membrane [16]–[18]. With the addition of ZTC, the membrane performance was shifted towards the upper bound and showed good improvement.
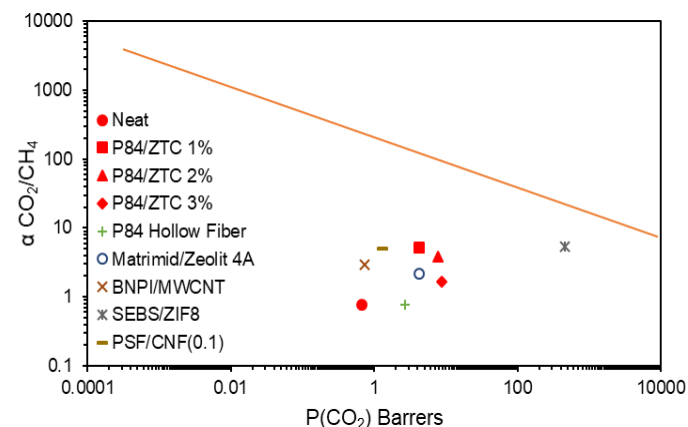

Figure 13 The membrane performance towards Robeson Upper Bound 2008.

CONCLUSION

In this study, a series of the loading composition of ZTC into P84 co-polyimide membrane has been studied. The ZTC has been successfully prepared via simple impregnation method of sucrose into zeolite-Y pore. The loading of ZTC improved the thermal stability of P84 co-polyimide. Microporous average pore size and regular pore structure of ZTC greatly improved the membrane permeability and selectivity. The optimum ZTC loading was at 1 wt%, where the fillers distributed homogeneously in the membrane and less agglomeration occurred. The significant boost both in permeability of CO_2 from 0.67 barrer to 4.26 and selectivity of CO_2/CH_4 from 0.76 to 5.23 with 1wt% ZTC loading was obtained. The organophilic properties of ZTC increased residual solvent on the membrane, thus improving the membrane permeability but reducing the selectivity. Higher ZTC loading was unnecessary since it tended to form agglomerate, which reduced the membrane selectivity performance. Overall, ZTC has a potential to be used as a filler in order to improve the gas permeation performance. To the best of our knowledge, this is the first research that utilized ZTC as filler in membrane for gas separation.

ACKNOWLEDGEMENT

REFERENCES

[1] T. Gunawan, R. Wijiyanti, and N. Widiastuti, "Adsorption–desorption of CO 2 on zeolite-Y-templated carbon at various temperatures," *RSC Adv.*, vol. 8, no. 72, pp. 41594–41602, 2018.

[2] C. Guan, K. Wang, C. Yang, and X. S. Zhao, "Characterization of a zeolite-templated carbon for H2 storage application," *Microporous Mesoporous Mater.*, vol. 118, no. 1–3, pp. 503–507, 2009.

[3] H. Nishihara and T. Kyotani, *Zeolite-Templated Carbon - Its Unique Characteristics and Applications*. Elsevier Ltd, 2012.

[4] H. Nishihara *et al.*, "High-pressure hydrogen storage in zeolite-templated carbon," *J. Phys. Chem. C*, vol. 113, no. 8, pp. 3189–3196, 2009.

[5] S. Choi *et al.*, "Large-scale synthesis of high-quality zeolite-templated

OPEN ACCESS Freely available online

carbons without depositing external carbon layers," *Chem. Eng. J.*, vol. 280, pp. 597–605, 2015.

[6] J. Shi, W. Li, and D. Li, "Rapidly reversible adsorption of methane with a high storage capacity on the zeolite templated carbons with glucose as carbon precursors," *Colloids Surfaces A Physicochem. Eng. Asp.*, vol. 485, pp. 11–17, 2015.

[7] X. H. Song, R. Xu, and K. Wang, "The structural development of zeolite-templated carbon under pyrolysis," *J. Anal. Appl. Pyrolysis*, vol. 100, pp. 153–157, 2013.

[8] A. Ebadi Amooghin, M. Omidkhah, and A. Kargari, "Enhanced CO_2 transport properties of membranes by embedding nano-porous zeolite particles into Matrimid®5218 matrix," *RSC Adv.*, vol. 5, no. 12, pp. 8552–8565, 2015.

[9] A. F. Ismail, D. Rana, T. Matsuura, and H. C. Foley, *Carbon-based Membranes for Separation Processes*. New York, NY: Springer New York, 2011.

[10] E. P. Favvas, E. P. Kouvelos, G. E. Romanos, G. I. Pilatos, A. C. Mitropoulos, and N. K. Kanellopoulos, "Characterization of highly selective microporous carbon hollow fiber membranes prepared from a commercial co-polyimide precursor," *J. Porous Mater.*, vol. 15, no. 6, pp. 625–633, 2008.

[11] H. H. Yong, H. C. Park, Y. S. Kang, J. Won, and W. N. Kim, "Zeolite-filled polyimide membrane containing 2,4,6-triaminopyrimidine," *J. Memb. Sci.*, vol. 188, no. 2, pp. 151–163, Jul. 2001.

[12] T. H. Weng, H. H. Tseng, and M. Y. Wey, "Preparation and characterization of multi-walled carbon nanotube/PBNPI nanocomposite membrane for H2/CH4 separation," *Int. J. Hydrogen Energy*, vol. 34, no. 20, pp. 8707–8715, 2009.

[13] W. S. Chi *et al.*, "Mixed matrix membranes consisting of SEBS block copolymers and size-controlled ZIF-8 nanoparticles for CO2capture," *J. Memb. Sci.*, vol. 495, pp. 479–488, 2015.

[14] A. Dehghani Kiadehi, A. Rahimpour, M. Jahanshahi, and A. A. Ghoreyshi, "Novel carbon nano-fibers (CNF)/polysulfone (PSf) mixed matrix membranes for gas separation," *J. Ind. Eng. Chem.*, vol. 22, pp. 199–207, 2015.

[15] N. Sazali, W. N. W. Salleh, and A. F. Ismail, "Carbon tubular membranes from nanocrystalline cellulose blended with P84 co-polyimide for H2 and He separation," *Int. J. Hydrogen Energy*, vol. 42, no. 15, pp. 9952–9957, 2017.

[16] N. H. Ismail, W. N. W. Salleh, N. Sazali, and A. F. Ismail, "Development and characterization of disk supported carbon membrane prepared by one-step coating-carbonization cycle," *J. Ind. Eng. Chem.*, vol. 57, pp. 313–321, Jan. 2018.

[17] W. N. W. Salleh, A. F. Ismail, T. Matsuura, and M. S. Abdullah, "Precursor selection and process conditions in the preparation of carbon membrane for gas separation: A review," *Sep. Purif. Rev.*, vol. 40, no. 4, pp. 261–311, 2011.

[18] E. P. Favvas *et al.*, "Gas permeance properties of asymmetric carbon hollow fiber membranes at high feed pressures," *J. Nat. Gas Sci. Eng.*, vol. 31, pp. 842–851, 2016.